APPLIED AND ENVIRONMENTAL MICROBIOLOGY, Aug. 2005, p. 4628–4637 Vol. 71, No. 8
0099-2240/05/$08.00+0 doi:10.1128/AEM.71.8.4628–4637.2005

Mobility of Protozoa through Narrow Channels

Wei Wang,[1] Leslie M. Shor,[1] Eugene J. LeBoeuf,[1] John P. Wikswo,[2] and David S. Kosson[1]*

Department of Civil and Environmental Engineering[1] and Vanderbilt Institute for Integrative Biosystems Research and Education,[2] Vanderbilt University, Nashville, Tennessee

Received 29 September 2004/Accepted 14 February 2005

Microbes in the environment are profoundly affected by chemical and physical heterogeneities occurring on a spatial scale of millimeters to micrometers. Physical refuges are critical for maintaining stable bacterial populations in the presence of high predation pressure by protozoa. The effects of microscale heterogeneity, however, are difficult to replicate and observe using conventional experimental techniques. The objective of this research was to investigate the effect of spatial constraints on the mobility of six species of marine protozoa. Microfluidic devices were created with small channels similar in size to pore spaces in soil or sediment systems. Individuals from each species of protozoa tested were able to rapidly discover and move within these channels. The time required for locating the channel entrance from the source well increased with protozoan size and decreased with channel height. Protozoa of every species were able to pass constrictions with dimensions equal to or smaller than the individual's unconstrained cross-sectional area. Channel geometry was also an important factor affecting protozoan mobility. Linear rates of motion for various species of protozoa varied by channel size. In relatively wide channels, typical rates of motion were 300 to 500 μm s^{-1} (or about 1 m per hour). As the channel dimensions decreased, however, motilities slowed more than an order of magnitude to 20 μm s^{-1}. Protozoa were consistently observed to exhibit several strategies for successfully traversing channel reductions. The empirical results and qualitative observations resulting from this research help define the physical limitations on protozoan grazing, a critical process affecting microbes in the environment.

Microscale heterogeneities of physical, chemical, and biological properties profoundly affect microbial communities in the environment (20). Soil or sediment is a physically and chemically complex material with nonuniform surface properties and a complex pore structure. Biological populations both are affected by the microscale heterogeneity of their habitat and contribute to the heterogeneity. For example, most soil bacteria are found in pores smaller than 10 μm and are absent in pores smaller than 0.8 μm (27). Predators of bacteria, including benthic protozoa, are also strongly influenced by sediment heterogeneity: protozoa are most commonly found near the redox discontinuity layer in sediments in the interstices of fine sands and are absent in fine-grained sediments or if a large proportion of clay is present (5). Chemical gradients including local regions of anoxia develop directly adjacent to active microbial communities, as nutrients are consumed at a rate faster than diffusion can replenish them.

Protozoan grazing has been shown to be an important factor in controlling the abundance and the activity of bacteria in the environment (8, 36). Protozoan grazing may select for bacterial populations based on size (1, 2, 7, 31), cell surface characteristics (23), or other bacterial properties. Predation has been shown to directly affect bacterial activity (25, 32). For example, the presence of protozoa can enhance net bacterial activity by improving the recycle rate of limiting nutrients (17, 36). The presence of protozoa has been demonstrated to enhance the rate of polyaromatic hydrocarbon degradation by bacteria (Taghon, personal communication) and mineralization of coal tar in the field (19). The effects of predation on bioremediation, however, have not been studied extensively.

Because predation by protozoa is a dominant factor controlling bacterial populations in nature (8, 14), it is natural that bacteria would employ various strategies to evade predation. For example, it has been suggested that bacterial cells adopting a very small or very large size (i.e., below 0.4 μm or greater than 2.4 μm) are protected to some extent from predation (24). Bacteria may also be resistant to predation by forming superstructures such as filaments (9) or flocs (10).

Another important means for predator avoidance may be nonuniform prey distribution within spatially heterogeneous soil or sediment (11, 12, 26, 28, 29, 36). Hassink et al. (11) examined microbial abundances in soils with different pore structures and found positive correlations between soil volume with pores between 0.2 and 1.2 μm in diameter and bacterial biomass and between soil volume with pores between 30 and 90 μm in diameter and nematode biomass (but no relationship was found between porosity and biomass of fungi or protozoa). Other authors have shown that bacteria tend to have a somewhat greater abundance in the fraction of soils with pore spaces smaller than 6 μm (27) and that such pores may protect bacteria from predation (12, 36). However, bacteria may tend to accumulate in smaller pores to be more protected from desiccation and exogenous water-soluble toxic substances in soils and sediments. Meanwhile, they face the added disadvantage of a more limited supply of nutrients diffusing into dead volumes (26, 27, 36).

The physical complexity of microbial habitats affects biological abundances, predation susceptibility, and concentrations and fluxes of various chemical species. Clearly there are a

* Corresponding author. Mailing address: Department of Civil and Environmental Engineering, Vanderbilt University, Box 1831 Station B, Nashville, TN 37235. Phone: (615) 322-1064. Fax: (615) 322-3365. E-mail: david.kosson@vanderbilt.edu.

TABLE 1. Properties of protozoan species[a]

Species	Length (μm)	Width (μm)	Height (μm)	Cross-sectional shape	Cross-sectional area (μm^2)	Doubling time (h)
Cyclidium sp.	26 ± 3	10 ± 1	10 ± 1	Circular	72.5	6
Uronema sp.	28 ± 6	9 ± 3	9 ± 3	Circular	63.9	6–7
HCIL	14 ± 2	8 ± 2	8 ± 2	Circular	48.4	5–7
E. plicatum	51 ± 5	32 ± 5	20 ± 2	Elliptical	497	19–24
E. vannus	82 ± 11	47 ± 7	26 ± 5	Elliptical	976	22–30
Keronopsis sp.	222 ± 66	35 ± 6		Irregular		53–60

[a] Protozoan dimensions were measured for 20 randomly picked individuals of each species. The values are given as means ± standard deviations (n = 20).

number of factors to consider when examining the effects of physical complexity on microbial populations. These factors are especially difficult to understand in complex systems, where competing factors exist simultaneously, or even in simplified microcosms or batch systems, where effects are observed at discreet intervals in the aggregate. Advances in microscope and computer technology make it possible to employ more direct real-time observations of microbial interactions. Direct observation enabled Wu et al. (37) to show that protozoa do graze on bacteria that are part of a filament. Further, they suggest the relative protective effect of forming filaments may have more to do with predation efficiency than contact probability, and the formation of flocs may not be a predator avoidance adaptation as much as a growth form made possible by enhanced nutrient conditions caused by the release of organic matter from grazing. In understanding the complex interactions of microorganisms, there is a need to control the many sources of complexity and to employ direct observations of individuals whenever possible.

Very few studies have directly observed and measured limitations on protozoan mobility in the absence of confounding physiochemical properties. One important exception is a recent study that investigated how brine channel geometry in sea ice affects the movement of small predators, including some protozoa (16). The study tested the relative abundance of microorganisms in liquid cultures with and without glass capillaries and evaluated the flexibility of predators' bodies to traverse narrowing capillary channels with diameters down to 69 μm. The maximum abundance of microorganisms occurred in capillaries with dimensions slightly smaller than the organism, perhaps because higher food concentrations cause predators to graze in small channels.

In this paper, we present a novel approach to studying the interactions of individual protozoa in spatially complex (but chemically uniform) engineered microenvironments. We employ direct observation of the mobility of six species of ciliated protozoa in microfluidic devices engineered with precise physical features 5 μm in size and smaller. Using these devices, we are able to show how individual protozoa locate and navigate along narrow channels of dimensions similar to those of pore spaces in the environment. Experiments were carried out to specifically test the effects of protozoan species, population densities, and channel dimensions and geometry on the mobility of protozoa. The results of this paper will be helpful in understanding the spatial limitations on bacterial grazing by protozoa in natural habitats.

MATERIALS AND METHODS

Protozoa cultures. The protozoan species used in the size exclusion experiment included *Euplotes vannus*, *Euplotes plicatum*, *Cyclidium* sp., *Uronema* sp. (clone BBcil), HCIL, and the *Keronopsis* sp. (see Table 1 and Fig. 1 for additional details on ciliate strains). *E. vannus* was obtained from the Culture Collection of Algae and Protozoa, Cumbria, United Kingdom. The other protozoa cultures were provided by Gary Taghon from the Institute of Marine and Coastal Sciences at Rutgers, The State University of New Jersey (the HCIL culture was initially provided to Gary Taghon by David Caron from the University of Southern California). The *Cyclidium* and *Uronema* isolates and HCIL are small hymenostomes. For estuarine sand microbiocenosis, they are one of the most important bacterivourous ciliates in surface layers and are known to play an important role in regulating bacterial populations (6). *E. plicatum*, *E. vannus*, and the *Keronopsis* sp. are hypotrich ciliates. *E. vannus*, in particular, is a widely distributed marine ciliate (18) and is commonly found in polluted environments (15). Bacterial predators such as *E. vannus* are especially well-suited to the microfluidic devices described here. They can feed on suspended bacteria when food are plentiful, but they are also well-adapted to feeding on surfaces (18).

The protozoa were maintained in solutions of artificial seawater for protozoa (ASWP). Solution composition per liter was 27.5 g instant ocean synthetic sea salts (Aquarium Systems, Inc, Mentor, OH), 0.5 g Tricine, 56.25 mg $NaNO_3$, 2.25 mg Na_2HPO_4, 1.88 mg K_2HPO_4 and 50 ml soil extract. The soil extract was prepared by mixing 105 g 1-cm sieved, dry soil and 660 ml deionized water and filtering the autoclaved supernatant with a 0.2-μm-pore-size GF/C glass fiber filter (Whatman Inc., Clifton, NJ). The final pH of the ASWP was adjusted to between 7.6 and 7.8 with 1 M NaOH, and the final salinity was 25‰ to reflect estuarine conditions.

Cultures were propagated by adding 1 ml of previous culture to 14 ml sterile ASWP in a 50-ml polystyrene tissue culture flask (Becton Dickinson, NJ). Several grains of sterile bolger rice were added as a substrate for bacterial growth, which in turn served as food for the protozoa. Cultures were incubated at room temperature (22°C) with exposure to indirect sunlight during the day and with the culture flask caps kept closed to prevent evaporation and concentration of the media. Once every 5 days the flasks were set upright and the caps were loosened to allow gas exchange.

Before each experiment, monoxenic protozoa cultures were obtained by a two-step filtration process. First, 15 ml of stationary-phase protozoa culture was filtered through a metal screen with a mesh size slightly larger than the protozoa cross-sectional area to remove large bacterial aggregates and rice debris. Then, the filtered culture was filtered again through a 5-μm polycarbonate membrane filter (Millipore) in a 15-ml sterile glass filter tower assembly (VWR International) and washed with sterile ASWP to flush away bacteria. Protozoa remaining on the filter were backwashed into a fresh culture flask with 15 ml sterile ASWP.

Determination of protozoan size. Protozoan length and width were measured for 20 random individuals in protozoa culture flasks by a calibrated Zeiss Axiocam video camera (Munich-Hallbergmoos, Germany) mounted on a fully automated Zeiss Axiovert 200 M microscope equipped with an image processing system (Axiovision 4.1, Carl Zeiss Vision GmbH, NY). This imaging system was also used for all other direct observations described in this manuscript. The heights of *E. plicatum* and *E. vannus* were also measured for 20 randomly selected individuals when they moved into or out of the observation plane. Since the height of the the *Cyclidium* and *Uronema* isolates and HCIL isolates were approximately the same as their widths, their cross-sectional areas were calculated based on a circular model. In contrast, the cross-sectional areas of *E. plicatum* and *E. vannus* were modeled as an ellipse due to the large difference between their widths and heights.

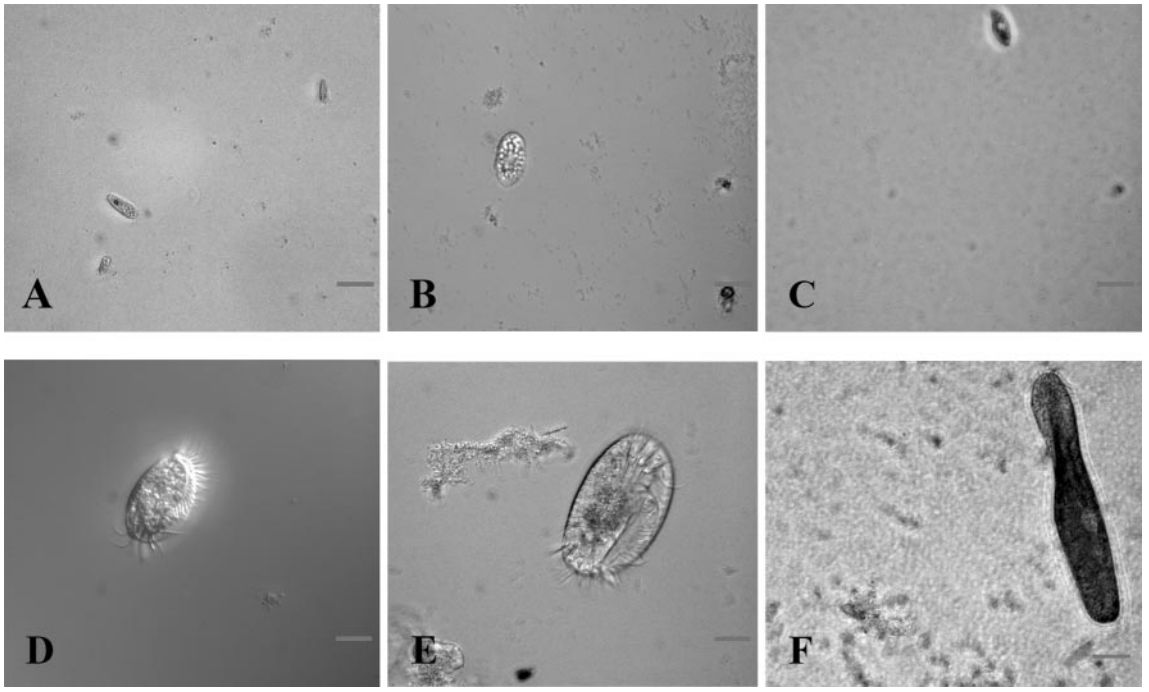

FIG. 1. Photographs of the six protozoan species tested. (A) *Cyclidium* sp.; (B) *Uronema* sp.; (C) HCIL; (D) *E. plicatum*; (E) *E. vannus*; (F) *Keronopsis* sp. (magnification, 400×, differential interference contrast phase). Scale bar, 20 μm.

Observation device design. Microfluidic devices were designed to determine the effect of physical constraints on protozoa mobility. The design consisted of two 4-mm-diameter cylindrical wells connected by an 11-mm-long channel (Fig. 2). Two designs (post-based and channel-based) were created to test the effect of constriction length on protozoa mobility. In the post-based design, the nominal channel width was kept constant at 100 μm, but 10 periodic sharp constrictions every 1 mm restricted the channel width from 50 μm to 5 μm. (Actual channel dimensions varied slightly due to uncontrollable differences in soft lithography fabrication conditions. See Table 2 for a list of actual channel dimensions.) These constrictions were created by 30-μm-wide posts that narrowed to sharp points on either side of the channel centerline. In the channel-based device, long constrictions were formed by reducing the entire channel width stepwise each 1 mm from 100 μm to 5 μm (Table 2). In both designs, constriction numbers and a length scale in micrometers past each constriction were incorporated into the design. This feature was helpful to track the position and swimming speed of individual protozoan.

The designs were drawn with AutoCAD 2002 (Autodesk, Inc.). From the AutoCAD drawings, Advanced Reproductions Corporation (North Andover, MA) created a reverse reading chromium mask used in the soft lithography procedure for microfluidic device fabrication.

Soft lithography techniques. Microfluidic devices were fabricated using standard soft lithography methods (30, 35, 38). All microfluidic device fabrication work was done in one of two class-100 clean rooms located at the Vanderbilt Institute for Integrative Biosystems Research and Education at Vanderbilt Uni-

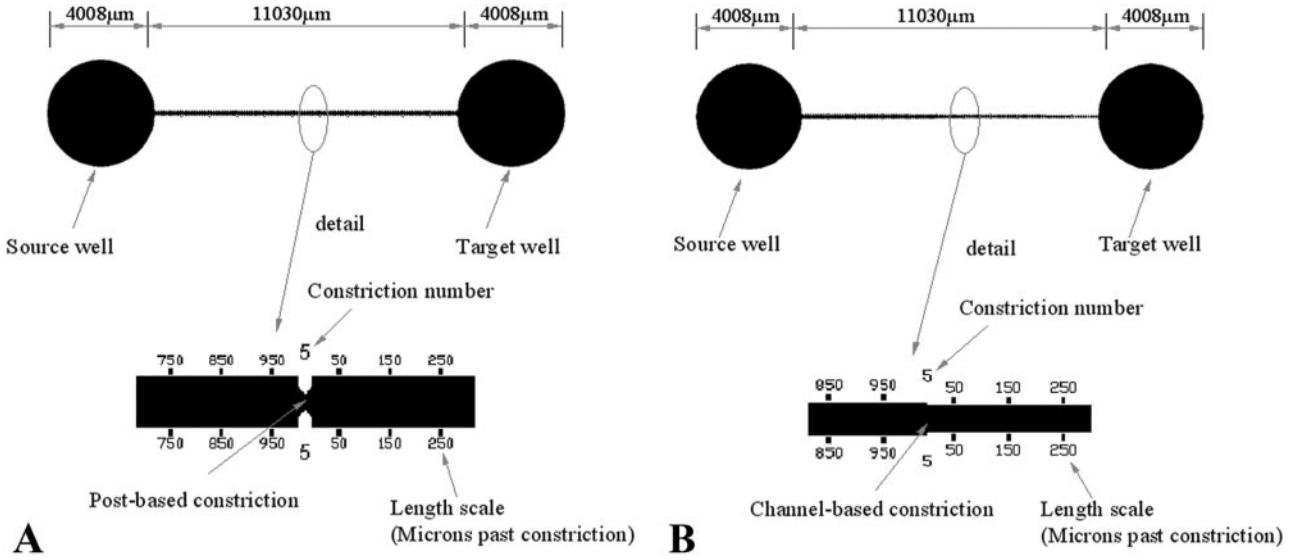

FIG. 2. Design of (A) post-based microchannel and (B) channel-based microchannel.

TABLE 2. Microchannel dimension parameters

Constriction no.	Post-based device constriction width (μm)				Channel-based device constriction width (μm)			
	Design width	Measured width at (μm)[a]			Design width	Measured width at (μm)[a]		
		38.5	19	5		38.5	19	5
Entrance	100	98.5	100.9	97.8	100	99.3	101.1	95.9
1	50	52.5	61.9	49.7	90	90.7	91.5	86.3
2	45	45.7	55.6	45.3	80	79.3	81.4	75.4
3	40	43.4	51.0	40.6	70	69.1	71.0	67.1
4	35	38.5	45.5	35.4	60	59.8	61.4	57.5
5	30	33.5	38.7	30.4	50	49.6	50.7	47.3
6	25	27.8	35.1	25.2	40	40.0	40.8	35.9
7	20	23.7	31.7	21.1	30	29.9	30.4	28.1
8	15	18.2	25.2	15.6	20	20.3	20.8	16.1
9	10	11.2	20.5	11.2	10	10.4	10.9	8.1
10	5	8.6	12.2	5.2	5	5.2	5.2	3.6

[a] The column headings 38.5, 19, and 5 represent the actual heights (in micrometers) of three different devices.

versity. First, a 2-inch-diameter, 289-μm-thick mechanical grade silicon wafer (University Wafer, South Boston, MA) was cleaned with ACS grade acetone, isopropyl alcohol, and ethyl alcohol in a spinner (model WS-400A-6NPP-LITE, Laurell Technologies Corporation, PA) at 4,000 rpm and baked at 200°C for 5 min (DataPlate digital hot plate, model PMC 720 Series). Approximately 2 ml of selected negative-tone photoresist (SU-8, MicroChem, Newton, MA) was dispensed onto the wafer on a spinner. The spin speed was first ramped to 500 rpm at 100 rpm/s acceleration to spread the photoresist. Then, to achieve the desired film thickness, the spin speed was ramped to a certain final speed at an acceleration of 336 rpm/s and held for a total of 30 seconds (Table 3).

Three photoresist heights (actual height: 5 μm, 19 μm, and 38.5 μm as measured by a digital profilometer) were created. Edge bead remover (MicroChem, Newton, MA) was applied to the edge of coated wafer at 500 rpm to remove the edge bead. The coated wafer was soft baked on a hot plate (Table 3). The substrate was then patterned by directed exposure to UV light through the customized chromium mask (MJB3 mask aligner, Karl Suss Inc., Germany). Following exposure, a post exposure bake was performed on a hot plate using a two-step procedure (Table 3). The patterned substrate was developed in SU-8 developer (MicroChem, Newton, MA) for 5 min to create a master mold. A controlled hard baking (Table 3) was carried on a hot plate to make the patterned structures on the master permanent.

Devices were cast in polydimethysiloxane (PDMS) (also called silicone rubber), $[Si(CH_3)_2\text{-}O\text{-}]_n$. PDMS has been shown to be an effective material to use in the fabrication of microfluidic devices (21). PDMS is an optically clear, flexible polymer that allows cells to be readily observed and also provides excellent permeability to gasses including oxygen and carbon dioxide (33). Given that the diffusivity of O_2 and CO_2 in PDMS at 35°C is reported to be 3.5×10^5 and 2.2×10^5 cm^2 s^{-1}, respectively (22), similar to the free diffusivity of these gasses in water (3), there is no problem supplying sufficient oxygen to maintain our aerobic cell cultures.

Sylgard 184 silicon elastomer and its curing agent (Dow Corning, Midland, MI) were mixed at a mass ratio of 10:1, degassed, and then poured over the master mold in plastic petri dishes (VWR International) and cured in an oven at 60°C for 2 h. After curing, the PDMS was peeled off the master and cut to appropriate size. Four-mm-diameter cylindrical wells were punched through the top of the device (the microchannels are imprinted into the bottom) with polished stainless steel tubing (Metric Type 316, outer diameter, 4 mm; inner diameter, 3.5 mm; McMaster-Carr, Atlanta, GA). The devices were cleaned with high-pressure liquid chromatography (HPLC)-grade methanol and dried in a nitrogen stream (class B, J&M Cylinder Gases Inc., Decatur, AL). Completed devices were pressed onto a clean microscope glass slide, such that the open flow channels lay between the PDMS block and the glass slide surface.

Size exclusion procedure. The microfluidic devices were first completely filled with 0.2-μm-filtered, sterile ASWP by application of vacuum. Approximately 15 individuals were then delivered into the devices by adding an appropriate volume of monoxenic protozoan culture (depending on the concentration of the cultures, this was typically about 10 μl). By running the "mark and find" program of Axiovision 4.1, the computer-controlled automatic stage of the microscope was moved to preselected coordinates so that photographs were taken of each segment of each device at 100× magnification every 5 min for 5 days. The time the first protozoa appeared in each progressively smaller channel segment was recorded by inspecting the photographs.

Scouting time experiment. To further investigate the effect of population density on the time for the first individual to enter the channel, or scouting time, different initial population densities of *E. vannus* ranging from 1 to 15 individuals (8 to 120 individuals ml^{-1}) from the same monoxenic culture were delivered separately to the introduction well of 15 different 38.5-μm-high size exclusion devices. *E. vannus* was selected for use in this study because its relatively long doubling time avoided the confounding effects of reproduction in most experiments. Photographs were taken at the channel opening every 1 second at 100× magnification until the first *E. vannus* entered the channel, and the total elapsed time was recorded.

Videomicroscopic observations. To examine the behavior of protozoa in size exclusion devices, live observations were performed by the previously described optical system. For the measurement of motility of protozoa in size exclusion devices, images were collected continuously at 2 frames s^{-1} at 400× magnification. Motility was determined by measuring the time required to swim the length of one segment (1,000 μm) of channel for each of at least three individual protozoa for a given channel dimension.

TABLE 4. Time to find channel opening from source well

Protozoan species	Time required in channels with indicated height					
	Post-based device			Channel-based device		
	38.5 μm	19 μm	5 μm	38.5 μm	19 μm	5 μm
Cyclidium sp.	30 s	2 min	41 min	30 s	1 min	26.5 h
Uronema sp.	2.5 min	4 min	19 h	2.5 min	5 min	22 h
HCIL	1 min	1.25 h	3.5 h	4 min	2.75 h	4.75 h
E. plicatum	1.75 h	112 h	N/A[a]	51 ± 1 h	N/A	N/A
E. vannus	1.75 h	31 ± 1 h	N/A	11 min	21.5 h	N/A
Keronopsis sp.	8 min	12 min	N/A	34 min	N/A	N/A

[a] N/A, stayed in the source well and did not enter the channels within 5 days.

RESULTS

Time for protozoa to find the channel. The time required for individual protozoa to locate and enter the channel from the source well, termed scouting time, varied as a function of protozoan size and channel dimensions (Table 4). For a given device, the scouting time tended to be shorter for the smaller protozoa. In the 38.5-μm-high post-based channel, small protozoa, including the *Cyclidium* and *Uronema* isolates and

TABLE 3. Microfabrication parameters

Channel height (μm)	Photoresist	Spin speed (rpm)	Soft bake time (min)		Exposure time (s)	Postexposure bake time (min)		Hard bake time (min)	
			Ramp from 25°C to 95°C	95°C		Ramp from 25°C to 95°C	95°C	Ramp from 25°C to 180°C	180°C
5	SU-8 2005	3,000	70	110	62	35	55	155	60
19	SU-8 2015	2,000	70	50	150	70	50	155	55
38.5	SU-8 2025	2,000	70	110	90	70	30	155	85

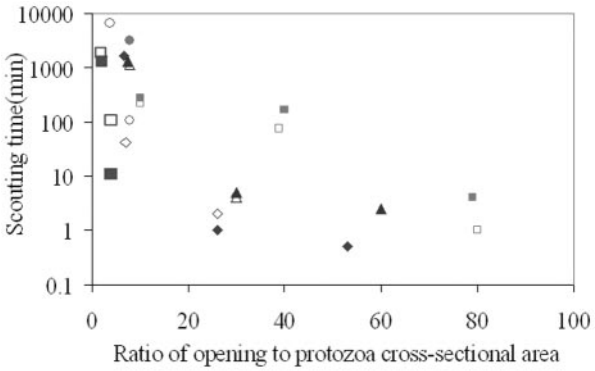

FIG. 3. Normalization of scouting time in post-based (open symbols) and channel-based devices (solid symbols) by ratio of channel opening to protozoan cross-sectional area. Symbols: *Cyclidium* sp. (diamonds), *Uronema* sp. (triangles), HCIL (small rectangles), *E. plicatum* (circles), and *E. vannus* (large rectangles).

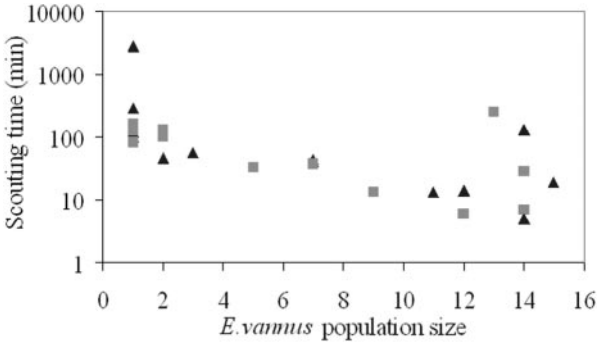

FIG. 4. Time required for *E. vannus* of different population densities to find the channel opening in post-based device (▲) and channel-based device (■).

HCIL, were able to locate the channel in less than 5 min after introduction. For the larger protozoa species *E. plicatum* and *E. vannus*, the scouting time increased to 1.75 h.

For a given species, larger channels tended to be located more quickly than smaller channels. For example, for HCIL in the channel-based device, the leader required 4 min to locate the channel of the 38.5-μm-high device, but 2.75 h and 4.75 h to locate the channel in 19-μm-high and 5-μm-high devices, respectively. The channel height had a statistically significant effect on the log of scouting time of small protozoa species (*Cyclidium*: $P = 0.04$; *Uronema*: $P = 0.028$; HCIL: $P = 0.005$). In contrast, for large protozoa (*E. plicatum* and *E. vannus*), there was a slight but insignificant difference for the log of scouting time between three channel heights (*E. plicatum*: $P = 0.55$; *E. vannus*: $P = 0.19$).

To explore if differences in scouting time can be explained by relative protozoan and channel cross-sectional area, the scouting times of all species in all devices were plotted against the ratio of the channel opening to the protozoa average cross-sectional area (Fig. 3). The results were somewhat scattered, although a general trend for decreasing scouting time with increasing ratio of opening to protozoa cross-sectional area is apparent ($P = 0.005$). However, it does not appear that differences between species in scouting time can be explained entirely by differences in physical size, leading to species-specific differences in how readily narrow channels are located and entered.

The influence of population density on scouting time was tested on *E. vannus* in 38.5-μm-high devices (Fig. 4, Table 5). There was a strong correlation between population size and log of scouting time ($P = 0.0001$). For example, comparing scouting time for populations of 1 versus 15 individuals of *E. vannus* in 38.5-μm-high post-based devices, the average scouting time decreased nearly two orders of magnitude from 1,218 min to 19 min. However, the reproducibility of the data was poor. All replicates had a relatively large standard deviation except the replicates for seven *E. vannus* in 38.5-μm-high post-based devices. There was no statistical difference between the two devices in the effect of population size on the log of scouting time.

Maximum penetration of protozoa. Once protozoa discovered the channel opening, to different extents they moved along progressively narrow channels. The measured parameter maximum penetration is defined as the smallest constriction size passed in the post-based device or the smallest channel traversed in the channel-based device for at least one individual of the species tested. Maximum penetration data are given in Table 6. Due to the different body sizes, small protozoa (the *Cyclidium* and *Uronema* isolates and HCIL) could pass smaller constrictions than large protozoa (*E. plicatum*, *E. vannus*, and the *Keronopsis* sp.). For example, in 38.5-μm-high channel-based devices, all small protozoan species passed each of the constrictions, including the narrowest, 5.2-μm-wide constriction, and reached the target well. In contrast, large protozoan species passed only some constrictions, becoming stuck in a channel of a certain width, preventing further movement toward the target well. The smallest traversed constrictions for *E. plicatum*, *E. vannus*, and the *Keronopsis* sp. were 19.8 μm, 20.3 μm, and 10.4 μm, respectively.

Channel height as well as width was also an important parameter affecting the movement of protozoa through narrow channels. Greater channel height resulted in decreased minimum constriction size that could be traversed by a given species in a given device type. In the case of *E. vannus*, an individual protozoon could pass through an 8.6-μm-wide constriction and reach the target well in 38.5-μm-high post-based devices. However, in post-based devices with a channel height of only 19 μm, the maximum penetration increased to 20.5 μm. In the 5-μm-high post-based channel, individual *E. vannus* could not enter a 97.8-μm-wide channel.

The effect of constriction length on maximum penetration was also tested. Constriction geometry was found to be an important factor limiting the mobility of protozoa in narrow channels. Protozoa were observed to be able to pass through smaller constrictions in post-based devices versus similarly sized constrictions in channel-based devices (Table 6). For example, in 19-μm-high post-based devices, individual *E. plicatum* organisms passed the 12.2-μm-wide constriction and reached the target well. In contrast, in channel-based devices with the same height, individuals of *E. plicatum* could not enter the 100.9-μm-wide channel.

Maximum penetration results were normalized by average protozoan cross-sectional area to determine if different species

TABLE 5. Population density-dependent scouting time of *E. vannus* in size exclusion devices

Post-based device					Channel-based device				
No. of *E. vannus* organisms	Population density (cells/ml)	No. of replicates	Avg scouting time (min)	SD (min)	No. of *E. vannus* organisms	Population density (cells/ml)	No. of replicates	Avg scouting time (min)	SD (min)
15	120	1	19	N/A[a]	14	112	2	18	15
14	112	2	69	91	13	104	1	252	N/A
12	96	1	14	N/A	12	96	1	6	N/A
11	88	1	13	N/A	9	72	1	13	N/A
7	56	2	42	1	7	56	1	37	N/A
3	24	1	58	N/A	5	40	1	33	N/A
2	16	1	46	N/A	2	16	4	111	13
1	8	5	1,218	1,433	1	8	4	132	35

[a] N/A, not applicable; the standard deviation for this condition could not be calculated since there is only one replicate.

possess similar abilities to traverse narrow channels relative to their size (Table 7). Because of the flexible bodies of the protozoan species tested and optical distortion imposed by the PDMS walls of microfluidic devices, it was impossible to measure the exact dimensions of protozoa inside size exclusion devices. The average dimensions of the protozoa listed in Table 1 were thus used to calculate protozoan cross-sectional areas. The relatively small standard deviations indicated the dimensions of protozoa from each species were quite uniform (Table 1).

In channel-based devices, the three small species of protozoa passed channels as small as 38% of the average cell's unconstrained cross-sectional area. But large protozoa were only able to traverse channels at or slightly smaller than their average unconstrained cross-sectional area. Protozoa moving through post-based devices could pass smaller obstacles with dimensions as small as 30% of the average protozoon's unconstrained cross-sectional area.

Motility. Linear rates of motion were measured for *Cyclidium* and *E. vannus*. In the 5-μm-high channel-based device, *Cyclidium* moved at an average speed ranging from 300 to 500 μm s^{-1} in wide channels with channel dimensions greater than 50 μm. However, as channel width decreased to 16.1 μm, the average rate of motion of individual *Cyclidium* organisms dropped to 97 μm s^{-1}. In 38.5-μm-high channel-based devices, *E.vannus* moved at an average velocity of 62 μm s^{-1} in the 49.6-μm-wide channel. The average motility of *E.vannus* decreased to 20 μm s^{-1} as individuals moved into narrow channels, where motion is constrained.

For individual *E. vannus* organisms in 38.5-μm-high post-based devices, the average rate of motion decreased from 298 μm s^{-1} to 164 μm s^{-1} after it passed the 18.2-μm-wide constriction, although the channel dimensions of the two segments were the same. The only apparent difference between the two segments was the prior presence and activity of individuals within the first segment and the absence of any prior protozoan activity in the second segment.

Video microscopic observations. By means of high-resolution video microscopy, we documented the behaviors of various protozoan species in several size exclusion devices. Protozoa were consistently observed to utilize several strategies for traversing narrow channels. All protozoa species tested alter their physical dimensions to some extent to pass constrictions (Fig. 5 and Fig. 6). The *Keronopsis* sp. organisms, in particular, have extremely flexible bodies and were able to easily change body shape and dimensions to traverse the constrictions (Fig. 6). For *E. vannus* and *E. plicatum*, whose body height is about 50% of their width, individuals altered their orientation, rotating to align their minimum cross-sectional dimension with the minimum dimension of the channel (Fig. 5). Other species, especially the *Cyclidium* and *Uronema* isolates and HCIL, used a corkscrew-like motion to pass constrictions much narrower than their own dimensions (Fig. 7). Although the behavior is more difficult to visualize in still photographs than by video, it is apparent from the three panels in Fig. 7 that dark regions within the leading cell move relative to the device as the cell rotates longitudinally as it propels itself forward.

All protozoan species tested except the *Keronopsis* sp. were also observed "getting a running start" in each device: a protozoon unable to pass a narrow constriction moved back in the

TABLE 6. Maximum penetration of single protozoa in size exclusion devices

Protozoan species	Smallest constriction passed in size exclusion devices (μm)					
	Post-based device			Channel-based device		
	H = 38.5 μm	H = 19 μm	H = 5 μm	H = 38.5 μm	H = 19 μm	H = 5 μm
Cyclidium sp.	<8.6[a]	<12.2[a]	<5.2[a]	<5.2[a]	<5.2[a]	8.1
Uronema sp.	<8.6[a]	<12.2[a]	<5.2[a]	<5.2[a]	<5.2[a]	8.1
HCIL	<8.6[a]	<12.2[a]	<5.2[a]	<5.2[a]	<5.2[a]	3.6
E. plicatum	9.4	<12.2[a]	>97.8[b]	19.8	>101.1[b]	>95.9[b]
E. vannus	<8.6[a]	20.5	>97.8[b]	20.3	20.8	>95.9[b]
Keronopsis sp.	<8.6[a]	<12.2[a]	>97.8[b]	10.4	>101.1[b]	>95.9[b]

[a] Passed last constriction and reached the target well. Number indicates narrowest constriction width.
[b] Stayed in the source well and did not enter the channels within 5 days. Number indicates width of channel opening.

TABLE 7. Ratio of channel to protozoan cross-sectional area for smallest constriction passed by an individual protozoan

Protozoan species	Ratio, channel: protozoan cross-sectional area					
	Post-based device			Channel-based device		
	H = 38.5 μm	H = 19 μm	H = 5 μm	H = 38.5 μm	H = 19 μm	H = 5 μm
Cyclidium sp.	<4.6[a]	<3.2[a]	<0.36[a]	<2.8[a]	<1.4[a]	0.56
Uronema sp.	<5.2[a]	<3.6[a]	<0.41[a]	<3.1[a]	<1.5[a]	0.63
HCIL	<6.8[a]	<4.8[a]	<0.54[a]	<4.1[a]	<2.0[a]	0.38
E. plicatum	0.73	<0.47[a]	>1.0[b]	1.50	>3.9[b]	>0.97[b]
E. vannus	<0.34[a]	0.40	>0.50[b]	0.80	0.41	>0.49[b]

[a] Passed last constriction and reached the target well. Number indicates ratio of the smallest constriction to protozoan cross-sectional area.
[b] Stayed in the source well and did not enter the channels within 5 days. Number indicates ratio of channel opening to protozoan cross-sectional area.

channel, appeared to speed up, and centered itself within the constriction using momentum. It often required several attempts to penetrate tiny channels.

Protozoa were also consistently observed to block rivals from the channel entrance in channel-based devices. When protozoa in the channel sensed other protozoa attempting to enter the same channel, they would move backward to the entrance until the intruders were expelled. This behavior occurred for all protozoan species examined except the *Keronopsis* sp. These observations may be the first documentation of competitive behavior between individual microorganisms.

DISCUSSION

Physical and chemical heterogeneities that exist on a spatial scale of millimeters to micrometers have been shown to influence microbial communities in natural habitats (5, 20). However, the effects of microscale heterogeneities cannot be replicated by conventional experimental techniques. Our experimental approach takes advantage of advances in soft lithography to fabricate engineered microfluidic devices to mimic the microscale physical complexity of porous media. Advanced microscopy and image processing software are also critical advances that allow the direct observation of the inter-

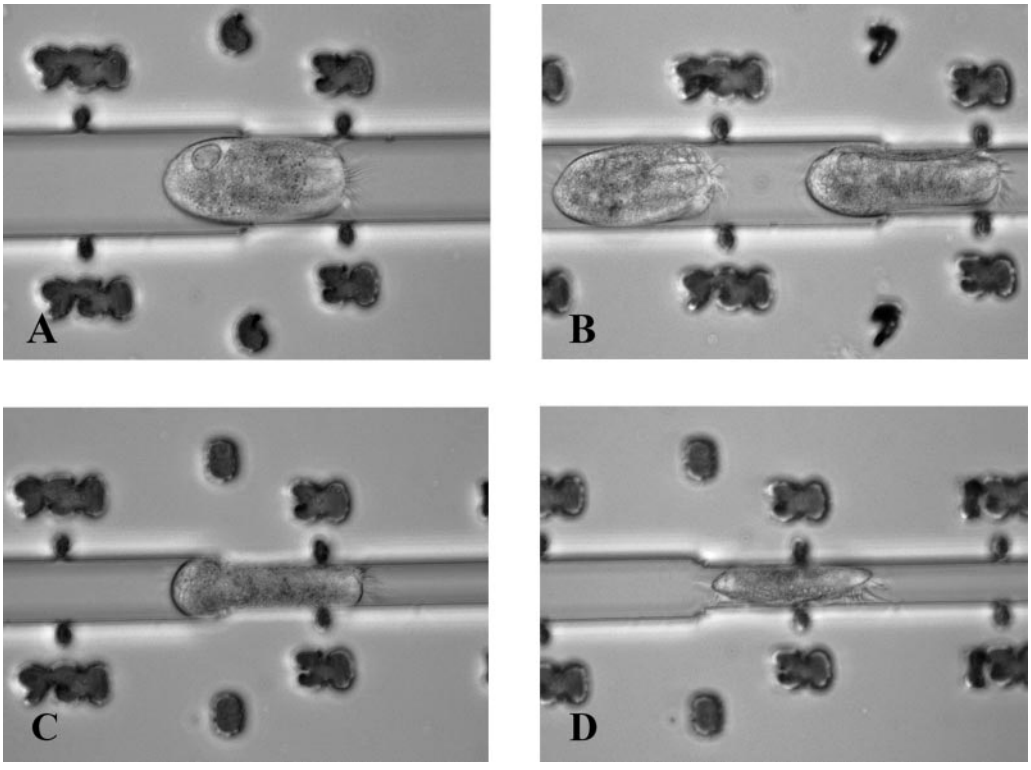

FIG. 5. Photographs of *E. vannus* in 38.5-μm-high channel-based device, passing (A) sixth constriction (40.0 μm wide), (B) seventh constriction (29.9 μm wide), (C and D) eighth constriction (20.3 μm wide). Note how the individual rotates between panels C and D to better match cell dimensions with channel dimensions.(magnification, 400×, bright-field phase).

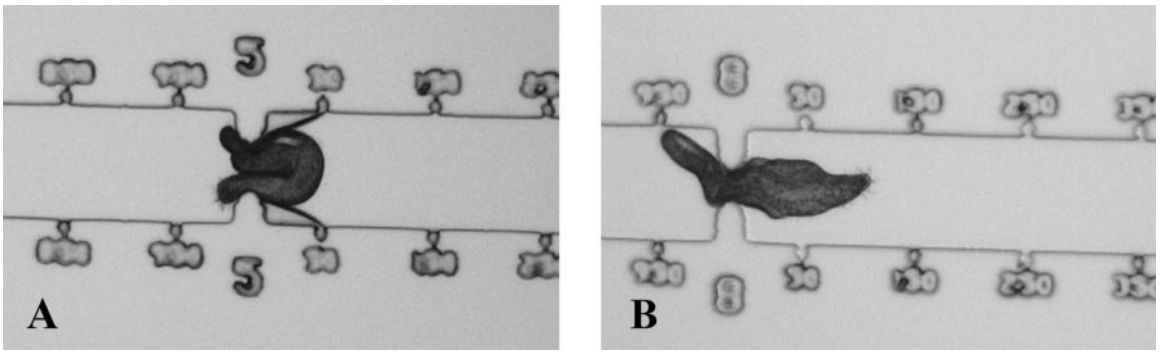

FIG. 6. Photographs of the *Keronopsis* sp. in 19-μm-high post-based device, deforming its body to pass (A) the fifth constriction (38.7 μm wide) and (B) the eighth constriction (25.2 μm wide). The two triangular areas in panel A immediately to the right of the constriction are air-filled regions (magnification, 100×, bright field).

actions of individual protozoa in spatially complex environments at the microscale.

Scouting time. The data from our size exclusion experiments show that protozoa in a relatively large reservoir readily locate channel openings possessing dimensions similar to naturally occurring pore spaces in soil or sediment. The channel openings in all devices are less than 0.003% of the total cross-sectional area of the entire source wells. Scouting time varies and is negatively correlated with increasing channel height and with decreasing protozoan size (Table 4). Normalization of the scouting times for all protozoan species and all devices by the ratio of the channel to the protozoan average cross-sectional area did not yield a consistent trend (Fig. 3), suggesting species-specific differences in channel-scouting times.

Holyoak and Lawler (13) examined protozoan predator (the predaceous ciliate *Didinium nasutum*) and prey (the bacterivorous ciliate *Colpidium striatum*) dispersal in an array of culture bottles (30-ml bottles linked by 0.2 cm-inner-diameter, 11.2-cm-long tubes) at different population densities (predator density: 32 to 645 ml^{-1}; prey density: 5.2 to 12.4 ml^{-1}). The dispersal rates were calculated as the proportion of individuals that dispersed from the source bottle to the target bottle per hour. They found that dispersal of predators and prey was not dependent on the density of their own populations, but that dispersal of prey was greater when predators were present. In our scouting time experiment, the dispersal rate of protozoa was quantified as the time required for the first protozoan individual to locate a channel from the source well. The results indicate that the scouting time for the leader individual is dependent on population size. Higher population density results in shorter scouting time (Table 5, Fig. 4).

We speculate that higher population size either makes protozoa more aggressive or increases the probability of contact with the channel entrance for any individual in a given time period. The current set of data derived from our scouting time experiment could not discriminate which mechanism dominates the scouting process. Further investigations concerning the influence of population size on scouting behavior is required.

Traversing of narrow channels. The results from size exclusion experiments revealed that protozoan species, constriction dimensions, and channel geometry all have an important effect on the mobility of protozoa. It confirms that the structure of porous substrates can strongly affect biological interactions (4, 5, 36).

Previous work has demonstrated that small pores may offer refuge for prey via size exclusion of predators, thus deterring predation. Krembs et al. (16) found that the diameter of the smallest glass capillaries containing euplotide ciliates was 12 μm. They also observed euplotide ciliates passed capillaries equal to 100% of their unflexed body diameter (while rotifers and turbellaria passed capillaries 57% and 60% of their unflexed body diameters, respectively). The minimum capillary diameter used to study body flexing, however, was 69 μm. Our work extends the previous results by investigating the mobility

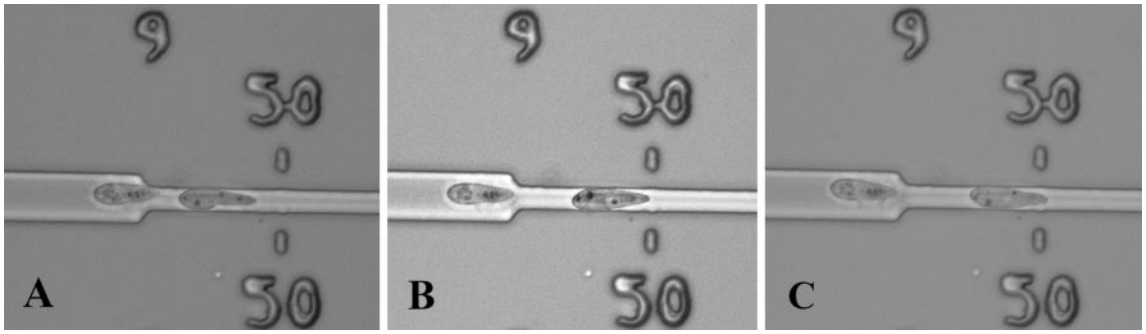

FIG. 7. Photographs of the *Uronema* sp. exhibiting corkscrew-like motion when it passes the 8.1-μm-wide channel in the 5-μm-high channel-based device. Note the rotation of dark spots within the leader cell (magnification, 400×, bright-field phase).

of protozoa in much smaller channels and also by investigating the effect of constriction geometry.

Other previous work from Wright et al. (36) suggested a minimum neck diameter of 6 μm provided significant protection to bacteria from predation by *Cyclidium steinii*. But the strain *Cyclidium steinii* they examined is 15 to 30 μm wide, larger than the small protozoan species (the *Cyclidium* and *Uronema* isolates and HCIL) examined in this paper. In our experiments, protozoa like the *Cyclidium* and *Uronema* isolates and HCIL could easily pass narrow constrictions with dimensions smaller than 5 μm, but these constrictions were effective in excluding larger predators such as *E. plicatum* and *E. vannus*. Our observations further indicate that protozoa were able to alter their physical dimensions to fit in small channels. Especially for those small protozoan species, the extreme plasticity of their body, relatively small body size, and fast swimming speed allowed them to gain access to very narrow long channels (as small as 30% of the culture's average sectional area) that are inaccessible to large protozoan species. Our results suggest that the activity of various protozoa may be differentially affected by various physical refuges in the environment, in part based on protozoan size. Accurately describing and predicting the effect of physical heterogeneity on predation pressure will require more extensive study.

The observed strategies adopted by protozoa, including corkscrew-like motion, "getting a running start," and blocking rivals from the entrance, can effectively help them traverse very small channels. Additional direct observations of individual protozoan behavior is required before we can begin to understand the myriad ways microorganisms interact with their natural environment.

Motility in narrow channels. Our unique experimental methods also allowed us to directly measure the motility of protozoa in narrow channels. Both the *Cyclidium* sp. and *E. vannus* exhibited decreased motility when they moved into progressively narrower segments of the channel-based device. Consistent with a previous study, this result suggests that pore constrictions may substantially diminish the rate of migration of predators versus mobility in larger pores (34). Further, individual *E. vannus* were observed to slow down when they moved in sequential segments of the post-based devices, even though the channel dimensions of each segment remained constant (only the width of the sharp constrictions dividing each segment decreased). We speculate that there may be a lingering chemical signal in the previously scouted channel that somehow induces individuals to exhibit more rapid movement. Another possible explanation is that squeezing through narrow constrictions may damage or otherwise affect the cilia of protozoa to some extent, which leads to the decrease in the rate of movement.

Additionally, small protozoa (the *Cyclidium* and *Uronema* isolates and HCIL) were consistently observed to move at a much higher velocity than large protozoa (*E. plicatum*, *E. vannus*, and the *Keronopsis* sp.) in the narrow channels of microfluidic devices. Fenchel (6), however, found that the swimming velocities of all ciliate species are constant at 1 mm s^{-1}, irrespective of body size. But these data were measured in bulk liquid, where no limitation of pore size is imposed on ciliates. In narrow channels, commonly found in natural estuarine habitats, the relatively small body size can gain more freedom of movement for small protozoan species, possibly resulting in relatively higher motility. The average rates of motion of individual protozoa in microfluidic devices presented here are much less than 1 mm s^{-1}.

Conclusions. In this paper, we stress the influence of spatial constraints on the mobility of six species of marine protozoa. We provide evidence that channel structures strongly affect the movement of protozoa. Protozoan behaviors at the pore scale including location of channel openings and navigation along narrow passages are reported for the first time. We also make quantitative measurements of the motility of protozoa in narrow channels. The empirical results and qualitative observations obtained in this study will be helpful in understanding the behavior of protozoa and the physical limitations on grazing by protozoa on bacteria in porous media. Our work will serve as the foundation for future studies that explore the response of protozoa to other environmental signals, including chemical gradients and fluid streaming. The ability to use microfluidic devices to control the physical and chemical environment while allowing quantitative measurements of protozoan activity suggests that this approach is ideally suited to determine many parameters that will be required for mathematical modeling of protozoan movement.

ACKNOWLEDGMENTS

This study was supported by grant 0120453 from the National Science Foundation and in part by the Vanderbilt Institute for Integrative Biosystems Research and Education through a grant from the Vanderbilt University Academic Venture Capital Fund.

We thank Gary Taghon and David Gruber for providing protozoan samples and technical assistance with culturing protozoa. We also thank Ronald Reiserer and Randall Reiserer for valuable advice and support with the device design and microfabrication process.

REFERENCES

1. **Christaki, U., J. R. Dolan, S. Pelegri, and F. Rassoulzadegan.** 1998. Consumption of picoplankton-size particles by marine ciliates: Effects of physiological state of the ciliate and particle quality. Limnol. Oceanogr. **43:**458–464.
2. **Chrzanowski, T. H., and K. Simek.** 1990. Prey-size selection by freshwater flagellated protozoa. Limnol. Oceanogr. **35:**1429–1464.
3. **Cussler, E. L.** 1997. Diffusion: mass transfer in fluid systems, 2nd ed. Cambridge University Press, Cambridge, England.
4. **Elliott, E. T., R. V. Anderson, D. C. Coleman, and C. V. Cole.** 1980. Habitable pore space and microbial trophic interactions. Oikos **35:**327–335.
5. **Fenchel, T.** 1969. The ecology of marine microbenthos. IV. Structure and function of the benthic ecosystem, its chemical and physical factors and the microfauna communities with special reference to the ciliated protozoa. Ophelia **6:**1–182.
6. **Fenchel, T.** 1987. Ecology of protozoa: the biology of free-living phagotrophic protists. Science Tech Publishers, Madison, Wis.
7. **Gonzalez, J. M., E. B. Sherr, and B. F. Sherr.** 1990. Size-selective grazing on bacteria by natural assemblages of estuarine flagellates and ciliates. Appl. Environ. Microbiol. **56:**583–589.
8. **Hahn, M. W., and m. G. Hofle.** 2001. Grazing of protozoa and its effect on populations of aquatic bacteria. FEMS Microbiol. Lett. **35**:113–121.
9. **Hahn, M. W., E. R. B. Moore, and M. G. Hofle.** 1999. Bacterial filament formation, a defense mechanism against flagellate grazing, is growth rate controlled in bacteria of different phyla. Appl. Environ. Microbiol. **65:**25–35.
10. **Hahn, M. W., E. R. B. Moore, and M. G. Hofle.** 2000. Role of microcolony formation in the protistan grazing defense of the aquatic bacterium *Pseudomonas* sp. MWH1. Microb. Ecol. **39:**175–185.
11. **Hassink, J., L. A. Bouwman, K. B. Zwart, and L. Brussaard.** 1993. Relationships between habitable pore-space, soil biota and mineralization rates in grassland soils. Soil Biol. Biochem. **25:**47–55.
12. **Heijnen, C. E., C. Chenu, and M. Robert.** 1993. Micro-morphological studies on clay-amended and unamended loamy sand, relating survival of introduced bacteria and soil structure. Geoderma **56:**195–207.
13. **Holyoak, M., and S. P. Lawler.** 1996. Persistence of an extinction-prone predator-prey interaction through metapopulation dynamics. Ecology **77:** 1867–1879.

14. **Jurgens, K., and C. Matz.** 2002. Predation as a shaping force for the phenotypic and genotypic composition of planktonic bacteria. Antonie Van Leeuwenhoek **81:**413–434.
15. **Kalavati, C., A. V. Raman, J. Vaidehi, and V. R. Bharathi.** 1997. Effects of pollution on planktonic ciliates in Visakhapatnam harbour. Indian J. Mar. Sci. **26:**68–73.
16. **Krembs, C., R. Gradinger, and M. Spindler.** 2000. Implications of brine channel geometry and surface area for the interaction of sympagic organisms in Arctic sea ice. J. Exp. Mar. Biol. Ecol. **243:**55–80.
17. **Kuikman, P. J., A. G. Jansen, J. A. Veen, and A. J. B. Zehnder.** 1990. Protozoan predation and the turnover of soil organic carbon and nitrogen in the presence of plants. Biol. Fertil. Soils **10:**22–28.
18. **Lawrence, J. R., and R. A. Snyder.** 1998. Feeding behaviour and grazing impacts of a Euplotes sp. on attached bacteria. Can. J. Microbiol. **44:**623–629.
19. **Madsen, E. L., J. L. Sinclair, and W. C. Ghiorse.** 1991. In situ biodegradation: microbiologal patterns in a contaminated aquifer. Science **252:**830–833.
20. **Marinelli, R. L., C. R. Lovell, S. G. Wakeham, D. B. Ringelberg, and D. C. White.** 2002. Experimental investigation of the control of bacterial community composition in macrofaunal burrows. Mar. Ecol. Prog. Ser. **235:**1–13.
21. **McDonald, J. C., and G. M. Whitesides.** 2002. Poly(dimethylsiloxane) as a material for fabricating microfluidic devices. Acc. Chem. Res. **35:**491–499.
22. **Merkel, T. C., V. I. Bondar, K. Nagai, B. D. Freeman, and I. Pinnau.** 2000. Gas sorption, diffusion, and premeation in poy(dimethylsiloxane). J. Polymer Sci. B Polymer Phys. **38:**415–434.
23. **Monger, B. C., M. R. Laudry, and S. L. Brown.** 1999. Feeding selection of heterotrophic marine nanoflagellates based on the surface hydrophobicity of their picoplankton prey. Limnol. Oceanogr. **44:**1917–1927.
24. **Pernthaler, J., B. Sattler, K. Simek, A. Schwarzenbacher, and R. Psenner.** 1996. Top-down effects on the size-biomass distribution of a freshwater bacterioplankton community. Aquat. Microb. Ecol. **10:**255–263.
25. **Posch, T., K. Simek, J. Vrba, J. Pernthaler, J. Nedoma, B. Sattler, B. Sonntag, and R. Psenner.** 1999. Predator-induced changes of bacterial size-structure and productivity studied on an experimental microbial community. Aquat. Microb. Ecol. **18:**235–246.
26. **Postma, J., C. H. Hok-A-Chin, and J. A. van Veen.** 1990. Role of microniches in protecting introduced *Rhizobium leguminosarum* biovar trifolii against competition and predation in soil. Appl. Environ. Microbiol. **56**:495–502.
27. **Ranjard, L., and A. S. Richaume.** 2001. Quantitative and qualitative microscale distribution of bacteria in soil. Res. Microbiol. **152:**707–716.
28. **Ronn, R., I. K. Thomsen, and B. Jensen.** 1995. Naked amoebae, flagellates, and nematodes in soils of different texture. Eur. J. Soil Biol. **31:**135–141.
29. **Schrag, S. J., and J. E. Mittler.** 1996. Host-parasite coexistence: the role of spatial refuges in stabilizing bacteria-phage interactions. Am. Nat. **148:**348–377.
30. **Shim, J., T. F. Bersano-Begey, X. Y. Zhu, A. H. Tkaczyk, J. J. Linderman, and S. Takayama.** 2003. Micro- and nanotechnologies for studying cellular function. Curr. Top. Med. Chem. **3:**687–703.
31. **Simek, K., and T. H. Chrzanowski.** 1992. Direct and indirect evidence of size-selective grazing on pelagic bacteria by freshwater nanoflageellates. Appl. Environ. Microbiol. **58:**3715–3720.
32. **Verhagen, F. J. M., and H. J. Laanbroek.** 1992. Effects of grazing by flagellates on competition for ammonium between nitrifying and heterotrophic bacteria in chemostats. Appl. Environ. Microbiol. **58:**1962–1969.
33. **Walker, G., M. Ozers, and D. Beebe.** 2002. Insect cell culture in microfluidic channels. Biomed. Microdevices **4:**161–166.
34. **Wallace, H. R.** 1971. The movement of nematodes in the external environment, p. 201–212. *In* A. M. Fallis (ed.), Ecology and physiology of parasites. University of Toronto Press, Toronto, Canada.
35. **Whitesides, G., E. Ostuni, S. Takayama, X. Jiang, and D. Ingber.** 2001. Soft lithography in biology and biochemistry. Annu. Rev. Biomed. Engr. **3:**335–373.
36. **Wright, D. A., K. Killham, L. A. Glover, and J. I. Prosser.** 1995. Role of pore size location in determining bacterial activity during predation by protozoa in soil. Appl. Environ. Microbiol. **61:**3537–3543.
37. **Wu, O. L. L., J. Boenigk, and M. W. Hahn.** 2004. Successful predation of filamentous bacteria by a nanoflagellate challenges current models of flagellate bacterivory. Appl. Environ. Microbiol. **70:**332–339.
38. **Xia, Y., and G. M. Whitesides.** 1998. Soft lithography. Annu. Rev. Materials Sci. **28:**153–184.